

# **Maintenance of the International Celestial Reference Frame**

S. Lambert, E. F. Arias

SYRTE, Observatoire de Paris, Université PSL, CNRS, Sorbonne Université, LNE  
61 av. de l'Observatoire, 75014 Paris, France

Published in IERS annual report 2018

## **1. Construction of the ICRF3**

Staff of the ICRS Centre at Paris Observatory worked on the construction of the Third Realization of the International Celestial Reference Frame (ICRF3) in the frame of activities of the Working Group on ICRF3 created at the XXVIII IAU General Assembly in 2012. The mission of the WG-ICRF3 concluded with the proposal to and adoption by the XXX IAU General Assembly in August 2018 of a catalog of radio source positions which realize the ICRS [Charlot et al. 2020]. Resolution B2 of the XXX IAU General Assembly [IAU 2019] resolves that as from 1 January 2019 ICRF3 is the fundamental realization of the International Celestial Reference System (ICRS). The ICRF3 is aligned onto ICRF2 [Fey et al. 2015] and represents a significant improvement in terms of radio source characterization, position accuracy and total number of sources. Objects in the new frame had been used to orientate the Gaia DR2 catalog onto the ICRS, as will be the case of the Gaia final catalog.

The ICRF3 is represented by three catalogs at bands S/X, K and X/Ka with 4536, 824 and 678 objects respectively [<http://iers.obspm.fr/icrs-pc/newwww/icrf>].

## **2. Monitoring of the ICRS**

Monitoring the ICRS is a mission of the IERS ICRS Centre. This includes verifications of the stability of the axes of the system materialized through the frame, identification of the possible deformations of the frame and tracking the astrometric evolution of its defining sources. Another aspect of this activity consists on the analysis of individual solutions submitted by the VLBI analysis centres to the International VLBI Service (IVS).

The IERS ICRS Centre at Paris Observatory developed the tools for determining the orientation of the axes, characterizing the deformations of the frame and analyzing the astrometric quality of radio source positions (Lambert 2014). Until mid-2018 these analyses were focused on the monitoring of the defining sources of the ICRF2 and contributed to selection of the defining sources of ICRF3.

### 3. Analysis of recent VLBI catalogs

#### 3.1. Data

We analyzed three catalogs submitted to the International IVS in 2018. The catalogs were respectively submitted by the Space Geodesy Centre of the Italian Space Agency (ASI/CGS; solution asi2018a), by Geoscience Australia (aus2018a) and by Paris Observatory (opa2018a). The aus2018a catalog was obtained with the OCCAM geodetic VLBI analysis software package (Titov et al. 2004), whereas the other two catalogs were obtained with Calc/Solve (Ma et al. 1986).

Since the catalogs were released before the date of adoption of the ICRF3, their individual frames had been oriented on ICRF2. However, in our analysis we have compared them to ICRF2 and to the catalog representing ICRF3 in the S/X bands (ICRF3X in this report) . The second Gaia data release (DR2; Prusti et al. 2016; Brown et al. 2016, 2018; Mignard et al. 2018) has been used also as a reference for comparison.

#### 3.2. Overview of the catalogs

The number of sources in each catalog, the mean epoch of the observations, and the median positional errors (for RA cos DEC, Dec, and for the error ellipse major axis) are reported in Table 1. The ASI solution contains the smallest number of sources. However, these are sources that have the best positional errors, and in consequence the median standard error is neatly smaller than that for the other catalogs. The standard error of the AUS positions is larger than that of OPA in a factor of 2.

	N	Epoch	E_RA*	E_Dec	E_EEMA
opa2018a	4160	2009.24	128.13	216.75	218.07
aus2018a	4267	2009.72	313.24	551.00	554.66
asi2018a	944	2009.24	39.36	48.40	49.48

Table 1. Statistic information of the catalogs here reported. N is the number of sources. The mean epoch corresponds to the average of the mean observational epochs of each source. N is the number of sources, E\_RA\*, E\_Dec are respectively the median standard errors in right ascension (scaled by cos dec) and in declination, E\_EEMA is the median major axis of error ellipses. Unit is  $\mu$ as.

The sky distribution of the radio sources in each catalog is plotted in Fig. 1 together with the distribution of the standard errors. In the sky maps, the color indicates the overall error computed as the major axis of the error ellipse, calculated using the correlation information between the coordinates as provided in the catalogs.

The error distribution, including that of the catalogs used as reference in the comparisons (ICRF2, ICRF3X and Gaia DR2) and the dependence of the error on the declination are displayed in Fig. 2, for which we took the running median error within windows of 15 degrees.

Fig. 2 shows a clear declination-dependent error for the individual catalogs and reflects the parameters of Table 1. Both AUS and ASI solutions show larger errors at mid- latitudes in the southern hemisphere, very probably due to the network asymmetry and the lower number of

observations in the south. The OPA solution presents a smoother deformation, almost in coincidence with that of ICRF3X. The improvement of ICRF3 with respect of ICRF2 is visible on the plots, both in precision and deformation. The Gaia DR2 solution does not show such systematic effects (the Gaia scanning law allows to cover both hemispheres symmetrically).

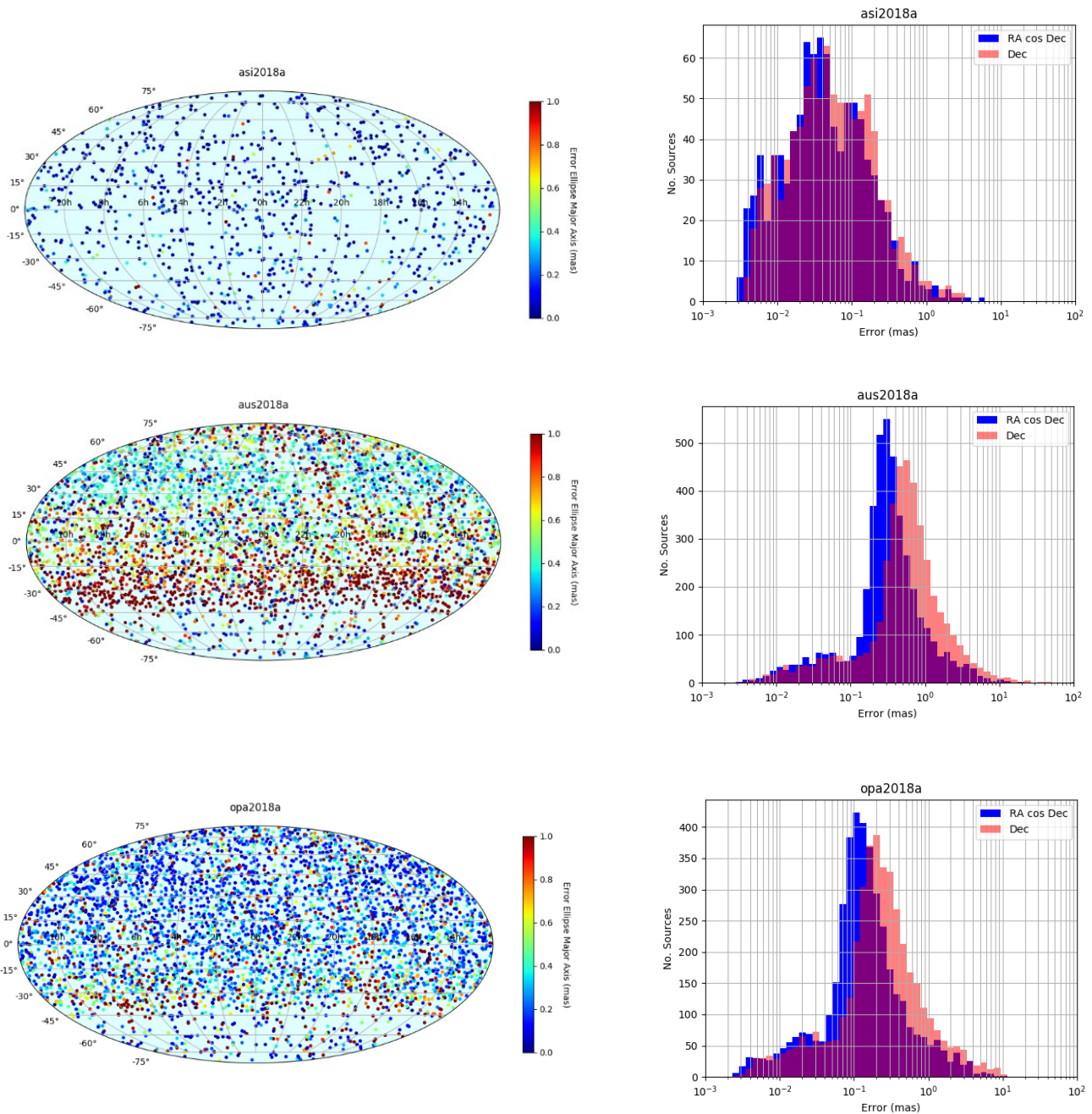


Figure 1. Left: sky distribution of the catalogs highlighting the overall positional error computed as the major axis of the error ellipse. Right: distribution of the standard errors on source position.

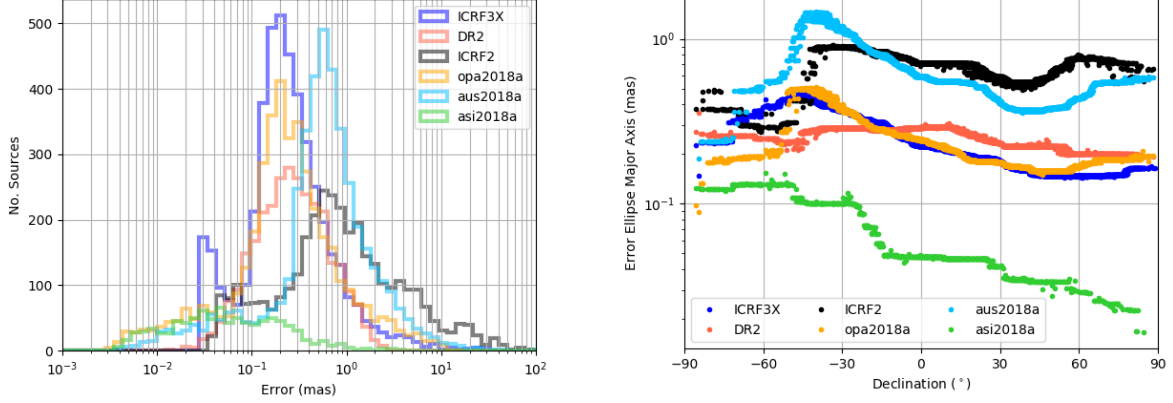


Figure 2. Left: overall comparison of the standard error distribution. Right: standard errors in source positions as a function of the declination smoothed by taking the running median within bins of 15 degrees.

### 3.3. Comparison with ICRF2, ICRF3 and Gaia DR2

Figure 3 displays the differences in declination between the catalogs and the references averaged within bins of 15 degrees. All three catalogs share the common feature of large (0.1-mas level) zonal differences with the ICRF2. A similar comparison with Gaia DR2 reveals that for ASI and OPA solutions the zonal deformation is much smaller, which is not the case for the AUS catalog. The same conclusion is valid for the zonal differences with respect to ICRF3X. Since Gaia DR2 is not expected to present zonal deformations, Fig. 3 suggests that recent VLBI catalogs are less deformed than ICRF2.

We used for the catalog comparisons the 16-parameter transformation accounting for rotations around the three axes, a glide, and degree-2 electric- and magnetic-type deformations (see e.g., Mignard and Klioner 2012). The coordinate differences  $\Delta\alpha$  and  $\Delta\delta$  between a catalog and a reference catalog read

$$\begin{aligned}
 \Delta\alpha \cos \delta &= R_1 \cos \alpha \sin \delta + R_2 \sin \alpha \sin \delta - R_3 \cos \delta - D_1 \sin \alpha + D_2 \cos \alpha + M_{20} \sin 2\delta \\
 &+ (E_{21}^{\text{Re}} \sin \alpha + E_{21}^{\text{Im}} \cos \alpha) \sin \delta - (M_{21}^{\text{Re}} \cos \alpha - M_{21}^{\text{Im}} \sin \alpha) \cos 2\delta \\
 &- 2(E_{22}^{\text{Re}} \sin 2\alpha + E_{22}^{\text{Im}} \cos 2\alpha) \cos \delta - (M_{22}^{\text{Re}} \cos 2\alpha - M_{22}^{\text{Im}} \sin 2\alpha) \sin 2\delta, \\
 \Delta\delta &= -R_1 \sin \alpha + R_2 \cos \alpha - D_1 \cos \alpha \sin \delta - D_2 \sin \alpha \sin \delta + D_3 \cos \delta + E_{20} \sin 2\delta \\
 &- (E_{21}^{\text{Re}} \cos \alpha - E_{21}^{\text{Im}} \sin \alpha) \cos 2\delta - (M_{21}^{\text{Re}} \sin \alpha + M_{21}^{\text{Im}} \cos \alpha) \sin \delta \\
 &- (E_{22}^{\text{Re}} \cos 2\alpha - E_{22}^{\text{Im}} \sin 2\alpha) \sin 2\delta + 2(M_{22}^{\text{Re}} \sin 2\alpha + M_{22}^{\text{Im}} \cos 2\alpha) \cos \delta,
 \end{aligned}$$

where  $\alpha$  and  $\delta$  are the coordinates of the object in the reference catalog. We used weighted least-squares to solve the system, with weights computed using the available covariance information (i.e., the standard errors on individual source coordinates and their correlation).

The values of the transformation parameters adjusted to the catalogs compared to the ICRF2, the ICRF3X and Gaia DR2 and their standard errors are reported in Fig. 4. The resulting statistics after removal of systematics are reported in Table 2. Figure 4 reveals that the results are similar independently from the set of sources used for the comparisons. The comparisons with ICRF2 show the presence of significant deformations, particularly D3 and E20, associated to the purely zonal deformations in  $\cos \delta$  and  $\sin 2\delta$ , respectively, along the polar axis of the celestial frame. These deformations range between 10 and 80  $\mu\text{as}$  depending on the individual solution. The analysis of the transformation onto ICRF3X shows that the only remaining significant deformations are those represented by D2 and D3; their values suggest that an offset between the equators of ICRF2 and ICRF3 could be the origin of this deformation. The transformation parameters with respect to Gaia DR2 show the presence of a rotation, certainly due to the fact that the individual VLBI solutions have been aligned to ICRF2 and Gaia's frame has been oriented onto ICRF3. Also deformations are visible dependent on declination, confirming the curves in Fig. 2, right.

Galactic aberration has been accounted for in the computation of ICRF3X source positions. A part of the detected zonal differences between ICRF3X and Gaia DR2 and the three analyzed catalogs is imputable to the uncorrected Galactic aberration that moves sources towards the Galactic centre following a glide of amplitude close to 5  $\mu\text{as}/\text{yr}$  (e.g., Kovalevsky 2003; Titov et al. 2011). Considering that the epochs of ICRF3 and Gaia DR2 are close (2015.0 and 2015.5 respectively), this effect is expected to be of around 30  $\mu\text{as}$  in D<sub>2</sub> and D<sub>3</sub> for the epochs of the individual catalogs (around 2009), explaining part of the results.

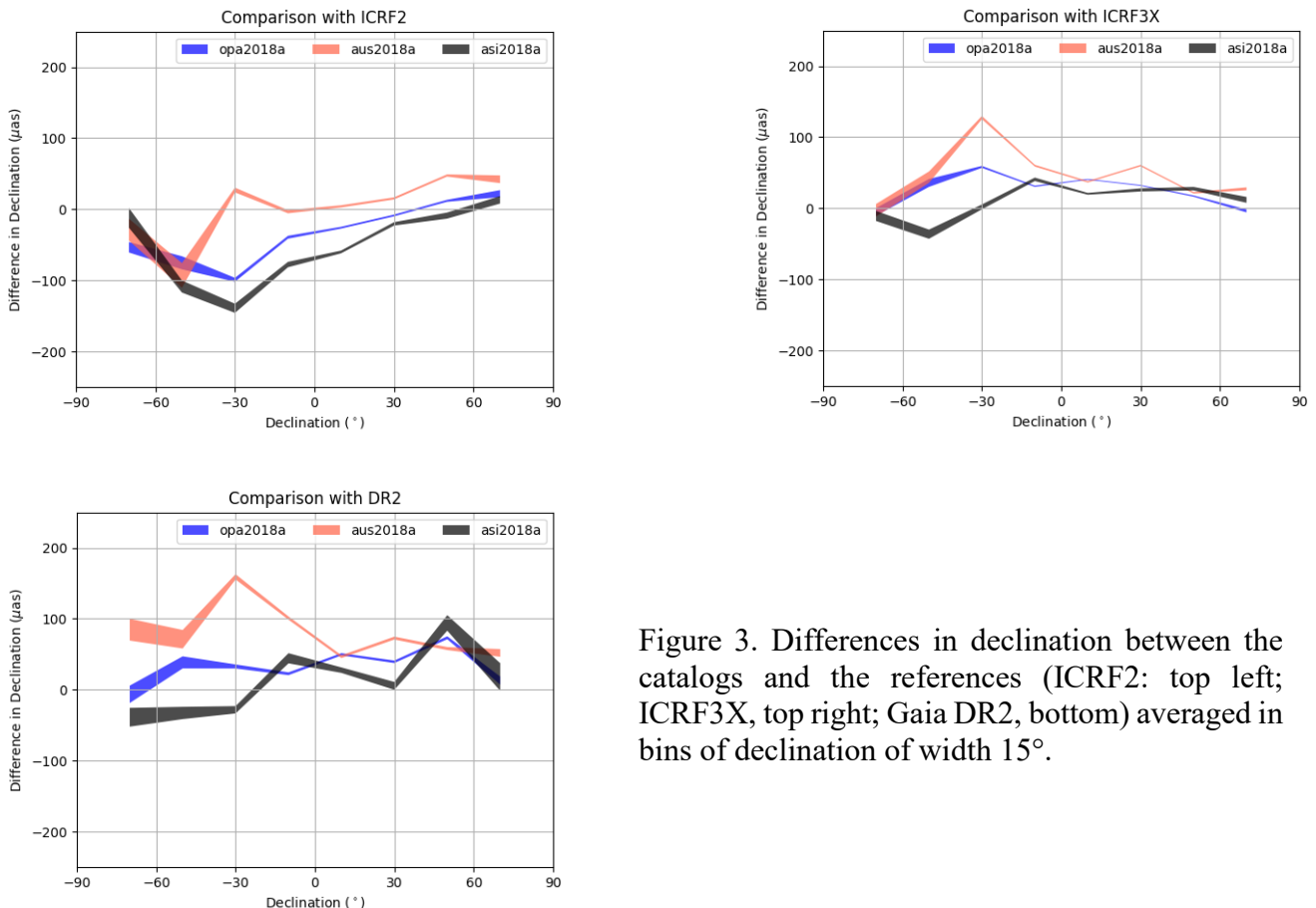


Figure 3. Differences in declination between the catalogs and the references (ICRF2: top left; ICRF3X, top right; Gaia DR2, bottom) averaged in bins of declination of width 15°.

Table 2. Statistics of the differences of the catalogs to ICRF2, ICRF3X and Gaia DR2 with different sets of common sources, and after removal of large-scale systematics. RA\* stands for RA cos\_dec. Unit is  $\mu$ as.

2a. With respect to ICRF2, N: number of sources common in ICRF2 and each individual catalog.

	N	Std_RA*	Std_Dec	Chi2_RA*	Chi2_Dec	Std_RA*	Std_Dec	Chi2_RA*	Chi2_Dec
opa2018a	3398	103.39	123.15	0.63	0.62	102.20	118.45	0.62	0.57
aus2018a	3359	124.76	146.58	0.71	0.70	124.46	145.09	0.71	0.68
asi2018a	893	96.73	122.20	1.57	1.87	91.27	110.24	1.40	1.52

2b. With respect to ICRF2, N: number of ICRF2 defining sources common in ICRF2 and each individual catalog.

	N	Std_RA*	Std_Dec	Chi2_RA*	Chi2_Dec	Std_RA*	Std_Dec	Chi2_RA*	Chi2_Dec
opa2018a	295	53.43	72.62	0.89	1.28	50.36	62.28	0.79	0.94
aus2018a	294	64.31	80.18	1.08	1.33	63.42	75.66	1.05	1.19
asi2018a	295	73.19	92.90	1.60	2.04	64.24	73.42	1.23	1.27

2c. With respect to ICRF2, N: number of sources common to all catalogs.

	N	Std_RA*	Std_Dec	Chi2_RA*	Chi2_Dec	Std_RA*	Std_Dec	Chi2_RA*	Chi2_Dec
opa2018a	727	62.76	82.07	0.76	0.96	60.61	73.90	0.71	0.78
aus2018a	727	86.84	101.77	1.15	1.19	86.36	99.84	1.14	1.14
asi2018a	727	94.45	119.26	1.61	1.94	88.44	105.94	1.41	1.53

2d. With respect to ICRF3X, N: number of sources common in ICRF3X and each individual catalog.

	N	Std_RA*	Std_Dec	Chi2_RA*	Chi2_Dec	Std_RA*	Std_Dec	Chi2_RA*	Chi2_Dec
opa2018a	4149	89.76	90.13	1.02	0.75	77.10	85.25	0.75	0.67
aus2018a	4234	117.42	127.78	1.07	1.01	107.53	121.35	0.89	0.91
asi2018a	941	64.11	70.28	1.63	1.67	57.91	66.81	1.33	1.51

2e. With respect to ICRF3X, N: number of ICRF3 defining sources common in ICRF3X and each individual catalog.

	N	Std_RA*	Std_Dec	Chi2_RA*	Chi2_Dec	Std_RA*	Std_Dec	Chi2_RA*	Chi2_Dec
opa2018a	303	51.13	37.52	1.52	0.71	23.39	24.00	0.32	0.29
aus2018a	300	61.85	62.67	1.66	1.51	39.76	45.27	0.69	0.79
asi2018a	273	46.65	47.30	1.28	1.17	38.55	42.17	0.87	0.93

2f. With respect to ICRF3X, N: number of sources common to all catalogs.

	N	Std_RA*	Std_Dec	Chi2_RA*	Chi2_Dec	Std_RA*	Std_Dec	Chi2_RA*	Chi2_Dec
opa2018a	727	56.28	43.87	1.55	0.78	31.16	32.51	0.48	0.43
aus2018a	727	72.74	73.05	1.80	1.55	54.31	60.33	1.00	1.05
asi2018a	727	60.66	67.34	1.65	1.74	53.54	63.62	1.28	1.55

2g. With respect to Gaia-DR2, N: number of sources common in DR2 and each individual catalog.

	N	Std_RA*	Std_Dec	Chi2_RA*	Chi2_Dec	Std_RA*	Std_Dec	Chi2_RA*	Chi2_Dec
opa2018a	2781	297.77	318.88	2.30	2.23	296.66	315.79	2.29	2.19
aus2018a	2816	344.25	358.40	1.89	1.68	342.91	355.05	1.87	1.65
asi2018a	775	218.50	222.77	2.47	2.65	214.37	218.13	2.38	2.54

2h. With respect to Gaia-DR2, N: number of sources common to all catalogs.

	N	Std_RA*	Std_Dec	Chi2_RA*	Chi2_Dec	Std_RA*	Std_Dec	Chi2_RA*	Chi2_Dec
opa2018a	727	209.01	218.12	2.60	2.80	207.00	212.41	2.55	2.66
aus2018a	727	230.90	239.01	2.53	2.58	228.00	232.25	2.47	2.43
asi2018a	727	211.60	219.81	2.42	2.70	207.84	214.90	2.34	2.58

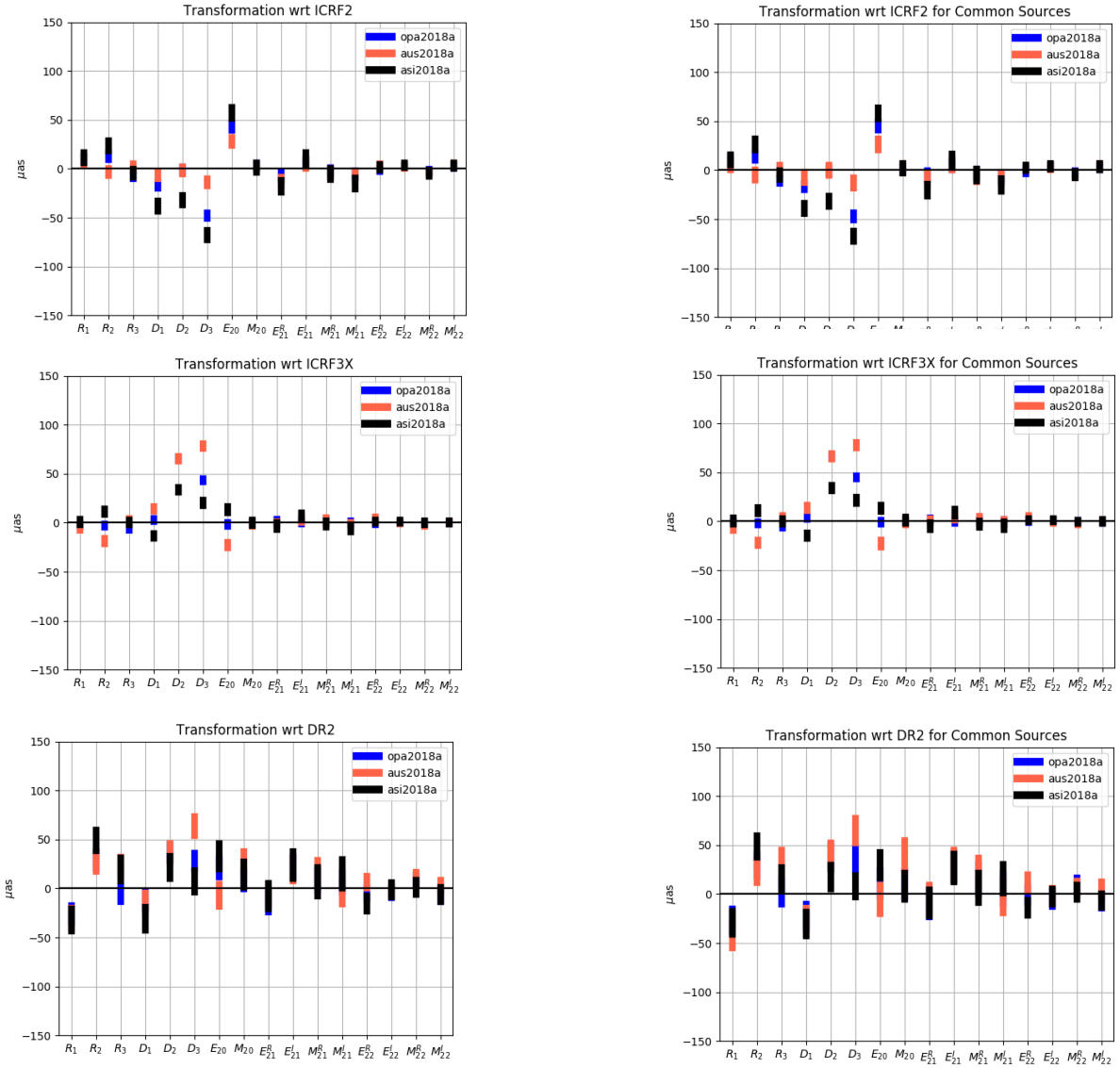


Figure 4. Transformation parameters between the catalogs under analysis and the reference frames (ICRF2: up, ICRF3X: middle, Gaia DR2: down). The plots on the left represent parameters computed with sources common to each individual catalog and the frame used as reference (from top to bottom they correspond to the statistics in tables 2a, 2d and 2g); the plots on the right represent parameters computed with sources common to all the catalogs involved in the comparisons, including the references (from top to bottom they correspond to the statistics in tables 2c, 2f and 2h).

### 3.4. Conclusions and recommendations

Three individual catalogs submitted to the IVS in 2018 are analyzed in this report. The axes of their frames are consistent with ICRF2 (to which they have been aligned) at the level of 30  $\mu\text{as}$  except for zonal deformations in  $\cos \delta$  and  $\sin 2\delta$  for which the amplitude of the difference reaches about 70  $\mu\text{as}$  (likely a combination of effects including the Galactic aberration and a network improvement). Compared to ICRF3X their axes are consistent to less 10  $\mu\text{as}$ , but zonal

deformations in  $\cos \delta$  peaking around  $70 \mu\text{as}$  are present. All three catalogs are consistent with Gaia DR2 within  $50 \mu\text{as}$ .

For a better evaluation of the consistency of the VLBI products and a better maintenance of the reference frame, we encourage analysis centres to submit solutions aligned to the new reference ICRF3. These catalogs should be as complete as possible, i.e., processing as much VLBI sessions as possible since 1979. Analysis strategies should be rigorously documented and motivated. The main points that will be scrutinized in the next reports will be the zonal systematics, their relation with the Galactic aberration, and the agreement with the current (DR2) and future releases of Gaia.

#### **4. References**

A. G. A. Brown, A. Vallenari, T. Prusti, J. H. J. de Bruijne, F. Mignard, R. Drimmel, C. Babusiaux, C. A. L. Bailer-Jones, U. Bastian, et al. Gaia Data Release 1. Summary of the astrometric, photometric, and survey properties. *Astronomy & Astrophysics*, 595:A2, Nov. 2016.

A. G. A. Brown, A. Vallenari, T. Prusti, J. H. J. de Bruijne, C. Babusiaux, C. A. L. Bailer-Jones, M. Biermann, D. W. Evans, L. Eyer, et al. Gaia Data Release 2. Summary of the contents and survey properties. *Astronomy & Astrophysics*, 616:A1, Aug. 2018.

P. Charlot, C. S. Jacobs, D. Gordon, S. B. Lambert, J. Boehm, A. de Witt, A. Fey, R. Heinkelmann, E. Skurikhina, O. Titov, E. F. Arias, S. Bolotin, G. Bourda, C. Ma, Z. Malkin, A. Nothnagel, R. A. Gaume, D. Mayer, and D. S. MacMillan. The third realization of the International Celestial Reference Frame by very long baseline interferometry. *Astronomy & Astrophysics*, (in preparation), 2020.

A. L. Fey, D. Gordon, C. S. Jacobs, C. Ma, R. A. Gaume, E. F. Arias, G. Bianco, D. A. Boboltz, S. Boeckmann, S. Bolotin, P. Charlot, A. Collioud, G. Engelhardt, J. Gipson, A.-M. Gontier, R. Heinkelmann, S. Kurdubov, S. Lambert, S. Lytvyn, D. S. MacMillan, Z. Malkin, A. Nothnagel, R. Ojha, E. Skurikhina, J. Sokolova, J. Souchay, O. J. Sovers, V. Tesmer, O. Titov, G. Wang, and V. Zharov. The Second Realization of the International Celestial Reference Frame by Very Long Baseline Interferometry. *Astronomical Journal*, 150:58, Aug. 2015.

International Astronomical Union. Transactions IAU, Vol. XXXB, Proc. of the XXX IAU General Assembly, August 2018 (Ed. Teresa Lago), 2019.

J. Kovalevsky. Aberration in proper motions. *Astronomy & Astrophysics*, 404:743–747, June 2003.

S. B. Lambert. Time stability of the ICRF2 axes. *Astronomy & Astrophysics*, 553:A122, 2013.

C. Ma, T. A. Clark, J. W. Ryan, T. A. Herring, I. I. Shapiro, B. E. Corey, H. F. Hinteregger, A. E. E. Rogers, A. R. Whitney, C. A. Knight, G. L. Lundqvist, D. B. Shaffer, N. R. Vandenberg, J. C. Pigg, B. R. Schupler, and B. O. Ronnang. Radio-source positions from VLBI. *Astronomical Journal*, 92:1020–1029, Nov. 1986.

F. Mignard and S. Klioner. Analysis of astrometric catalogues with vector spherical harmonics. *Astronomy & Astrophysics*, 547:A59, 2012.

F. Mignard, S. A. Klioner, L. Lindegren, J. Hernandez, U. Bastian, A. Bombrun, D. Hobbs, U. Lammers, D. Michalik, et al. Gaia Data Release 2. The celestial reference frame (Gaia-CRF2). *Astronomy & Astrophysics*, 616:A14, 2018.

T. Prusti, J. H. J. de Bruijne, A. G. A. Brown, Vallenari, A., Babusiaux, C., Bailer-Jones, C. A. L., Bastian, U., Biermann, M., Evans, D. W., et al. The Gaia mission. *Astronomy & Astrophysics*, 595:A1, 2016.

O. Titov, V. Tesmer, and J. Boehm. OCCAM v.6.0 Software for VLBI Data Analysis. In N. R. Vandenberg and K. D. Baver, editors, *International VLBI Service for Geodesy and Astrometry 2004 General Meeting Proceedings*, page 267, June 2004.

O. Titov, S. B. Lambert, and A.-M. Gontier. VLBI measurement of the secular aberration drift. *Astronomy & Astrophysics*, 529:A91, May 2011.